Development of a gemcitabine-polymer conjugate with prolonged cytotoxicity against a pancreatic cancer cell line

Fanny Joubert,*[,†] Liam Martin,[‡] Sébastien Perrier,[‡,§] George Pasparakis*[,†]

[†]UCL School of Pharmacy, 29-39 Brunswick Square, WC1N 1AX London, UK
[‡]Department of Chemistry, University of Warwick, Gibbet Hill Road, Coventry CV4 7AL, UK
[§]Faculty of Pharmacy and Pharmaceutical Sciences, Monash University, 381 Royal Parade, Parkville, Australia

ABSTRACT: Gemcitabine (GEM) is a nucleoside analogue of deoxycytidine with limited therapeutic efficacy due to enzymatic hydrolysis by cytidine deaminase (CDA) resulting in compromised half-life in the bloodstream and poor pharmacokinetics. To overcome these limitations, we have developed a methacrylate-based GEM-monomer conjugate, which was polymerized by reversible addition fragmentation chain transfer (RAFT) polymerization with high monomer conversion (~ 90%) and low dispersity (< 1.4). The resulting GEM-polymer conjugates were found to form well-defined sub-90 nm nanoparticles (NPs) in aqueous suspension. Subsequently, the GEM release was studied at different pH (~7 and ~5) with and without the presence of an enzyme, Cathepsin B. The GEM release profiles followed a pseudo zero-order rate and the GEM-polymer conjugate NPs were prone to acidic and enzymatic degradation, following a two-step hydrolysis mechanism. Furthermore, the NPs exhibited significant cytotoxicity *in-vitro* against a model pancreatic cell line. Although, the half-maximal inhibitory concentration (IC_{50}) of the GEM-monomer and -polymer conjugate NPs was higher than free GEM, the conjugates showed superiorly prolonged activity compared to the parent drug.

In 2014 cancers caused the death of over 163,000 people in the UK, of which 8,800 people died from pancreatic cancer, which now accounts as the fifth most lethal cancer with an estimated overall survival rate of 5-6%[1] after 5 years. In most cases, pancreatic tumors are not resectable (~80%[2]) and hence chemotherapy is required. The first-line chemotherapeutic drug for pancreatic cancer is gemcitabine (GEM), a nucleoside analogue of deoxycytidine which improves the overall survival rate to 21% after 5 years[3]. Despite its clinical potency, GEM is well known to be metabolically unstable due to its rapid deamination in the blood stream, primarily by cytidine deaminase, resulting in rapid clearance trough the kidneys[4-5]. Furthermore, its poor cell membrane permeability, predominantly *via* the human equilibrative type transporters (hENT1, hENT2, and hCNT3[6-9]) compromises its cytotoxic activity. To compensate for these limitations clinically, a high dose of GEM (1,000 mg/m^2) is administered which is often accompanied by severe side effects for patients such as breathlessness, neutropenia, nausea, and kidney failure[10]. In recent years, chemical derivatization of GEM at the 5'-OH or the primary amino position have been reported to formulate lipophilic or soluble GEM derivatives with interesting pharmacological properties that often outcompete the parent drug[11-14]. For example, the formulation of GEM (and other potent anticancer agents) in the form of water soluble macromolecular or self-assembled constructs has been shown to improve the blood circulation times which in turn increases their passive accumulation at the tumor sites *via* the enhanced permeation and retention effect[15-16], protects the drugs from premature hydrolysis and/or deactivation and allow for further conjugation with targeting ligands that exert active targeting properties at the cellular level[17-18].

Of particular interest is the construction of polymeric prodrugs, where GEM is attached *via* a pre[19, 20] or post[19, 21-25] polymerization functionalization procedure. The latter approach is synthetically more accessible (see for example[26]), however, it often produces ill-defined end-products with non-quantitative drug functionalization or generates side-products across the polymer backbone. On the other hand, the synthesis of polymerizable drug monomers is aesthetically and practically more appealing from various viewpoints (i.e. polymerizable synthons allow for unprecedented synthetic versatility in terms of co-monomer combination capacity, they lead to the production of well-defined final polymers, and eliminate the need for further reaction/purification steps), and has been recently exploited in the synthesis of polymer-drug conjugates[27-28]. Different synthetic approaches on polymerizable GEM synthons have been reported in the literature. Of particular interest are the works by Kopecek *et al.*[29-31] that synthesized methacrylamide-based GEM monomers containing an enzyme-sensitive oligopeptide linker, while Lin *et al.*[32] reported the enzymatic synthesis of acrylate-based GEM monomers. More recently, Xiao *et al.*[33] also reported on acrylate GEM derivatives with an acid-labile silyl ether bond[34]. Indeed, from these studies it is shown that it is possible to control various parameters such as the rate of drug loading per particle/conjugate, the rate of hydrolysis and the copolymerization with other monomers for the construction of higher-order structures. Herein we report a facile synthesis of a methacrylate-based GEM-monomer conjugate that can be directly polymerized by the RAFT process. RAFT polymerization enables good control over the molecular weight and molecular weight distribution of the final polymer, properties that are key for bioapplications.[35] In addition, we demonstrate that the polymer forms well-defined nanoparticles with very high drug loading ratio and interestingly, it exhibits superiorly prolonged efficacy compared to the parent drug *in vitro*.

The GEM-monomer conjugate **3** was prepared in a direct one–step amidation reaction by coupling GEM.HCl **1** with mono-2-methacryloyloxy ethyl succinate **2** (Scheme 1a) at room temperature for 48 h in the presence of 1-hydroxybenzotriazole (HOBT), 1-(3-dimethylaminopropyl)3-ethylcarbodiimide hydrochloride (EDC) and pyridine. The crude product was purified by column chromatography and was isolated in adequate yield of 45%. With the use of ^{1}H-^{13}C NMR correlation spectra (Figure S1) it was possible to trace the covalent linkage between GEM and mono-2-methacryloloxy ethyl succinate: The peak δ_C ~ 172.7 ppm assigned to the carbonyl group correlates to three different protons δ_H =11.08, 2.71 and 2.59 ppm which are assigned to the -NH, -CH_2-C$\underline{H}_2$-C(=O)-NH- and -C$\underline{H}_2$-CH_2-C(=O)-NH-

Scheme 1. Synthesis of GEM-monomer conjugate and its RAFT polymerization[a]

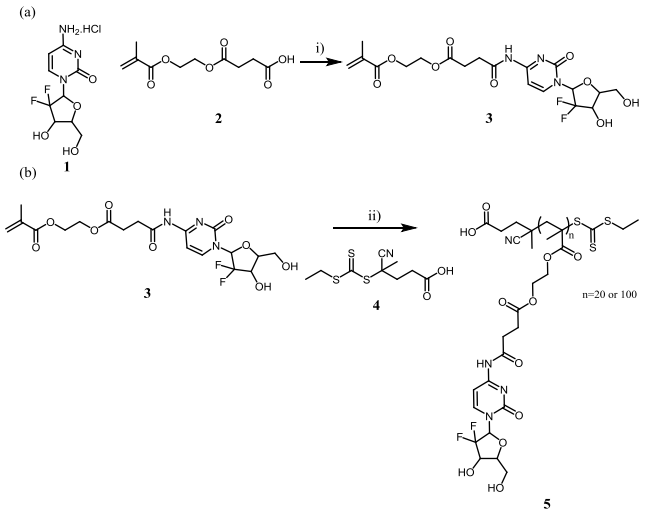

[a](a) Synthesis of methacrylate-based GEM-monomer conjugate **3**: i) HOBT/EDC, pyridine, 72 h, at room temperature, DMF, under positive Ar (b) RAFT polymerization conditions of **3** using a trithiocarbonate **4** as CTA: ii) 4 h at 70 ˚C in DMF under positive N_2

groups respectively, which confirm the formation of the amide derivative and the complete absence of the ester side-product derivative (via possible attachment to the primary alcohol of GEM). The formation of the primary amide product was also confirmed by LC-MS with a found m/z value of 476.10 g/mol and the detection of a single signal peak on the LC spectrum which is indicative of the complete absence of impurities. The GEM-monomer conjugate **3** was polymerized by RAFT at 70 ˚C, using (4-cyanopentanoic acid)ylethyl trithiocarbonate chain transfer agent **4,** and 4,4′-azobis(4-cyanovaleric acid) (ACVA) as initiator at a CTA/initiator ratio set to 5 (Scheme 1b) and an initial monomer concentration of 0.5 mol/L. The ^{1}H NMR spectrum of a representative polymer product with degree of polymerization (DP) 20 is shown in Figure 1. The chemical shift δ_H ~ 11.04 ppm was assigned to the proton of the amide group, the peaks at δ_H ~ 8.20 and 6.29 ppm to the protons of the methine groups of the six-membered ring and the peaks at δ_H ~7.22, 6.16 and 5.24 ppm to the protons of the methine group of the five-membered ring of GEM. Furthermore, the set of peaks at the δ_H ranging from 4.08 to 4.20 ppm were assigned to the protons of the methylene groups of the side chain (-O-CH_2-) and the secondary alcohol at the 3'-position. Moreover, the set of peaks ranging from δ_H ~ 3.66 to 3.89 ppm were assigned to the protons of the methylene group (-CH_2-OH) and the primary alcohol at the 5'-position. The peaks δ_H ~ 2.71 ppm and 2.59 ppm were assigned to the protons of the methylene groups which are adjacent to the amide and ester group respectively. The broad peak at δ_H ~ 1.81 ppm was assigned to the protons of methylene group defining the methacrylate backbone of the polymer and the set of peaks with δ_H ranging from 0.78 to 0.74 ppm were assigned to the protons of the methyl group. Despite the low DP of the examined polymer sample, it was not possible to trace the corresponding peaks of the CTA as they overlapped with other residues of the bulky polymer chain. Therefore, the M_n of the polymer could not be estimated by NMR spectroscopy. Furthermore, the kinetics of the RAFT polymerization targeting a DP of 100 repeating units was investigated as a model polymerization reaction (Figure 2a). The rate of the monomer conversion versus time was first-

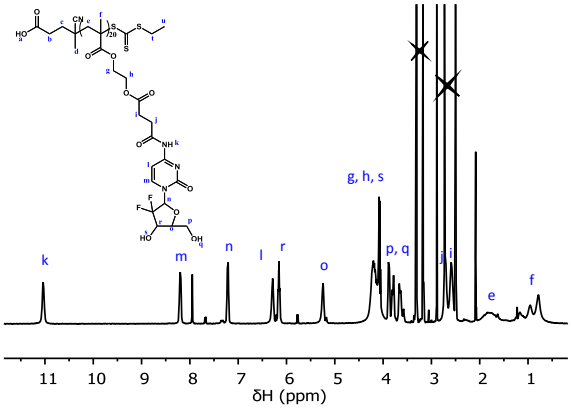

Figure 1. ^{1}H NMR (400 MHz, DMSO-d_6) spectrum of the GEM-polymer conjugate **5**; DP 20 (× designates the NMR and residual solvents peaks).

order after a retardation period of 1 h. Furthermore, the M_n increased linearly with monomer conversion (Figure 2b) although the theoretical and experimental values were significantly different. For monomer conversion lower than 50%, the experimental values were higher than the theoretical ones whereas they were slightly lower than the theoretical ones for monomer conversion above ~ 60%. This difference can be attributed to the hybrid behavior of the RAFT process, that is typically observed when a CTA of lower chain transfer constant to the monomer (which we would expect for this system between the trithiocarbonate CTA and the bulky methacrylate GEM monomer[36-37]). This led to some uncontrolled free radical polymerization in the early stage of the polymerization resulting in the formation of some dead chains (corresponding to the shoulder observed at low conversions, 1-2h, Figure 2c). When the controlled system takes over, the dead chains are left behind and the main chain population shifts to higher molecular weights, resulting in a lower than expected M_n, due to low molecular weights tail from dead chains. Eventually, the $Đ_M$ increased from 1.18 up to 1.36 with the increase of the monomer conversion. After 4 h, a monomer conversion of 90% was reached and a $Đ_M$ value of 1.25 was obtained. After 8 h, the $Đ_M$ increased to 1.36 due to termination reactions and possible loss of control of the polymerization. Due to this all subsequent polymerization times were fixed at 4 h. To investigate the influence of the DP on the dispersity, polymers of different chain lengths were prepared. DP of 10, 20 and 50 were chosen and the polymerization was run in DMF at 70 ˚C, for 4 h. A high monomer conversion around 90% was obtained with dispersity values lower than 1.2 indicating good control of the polymerization reaction (Figure 2d).

Interestingly, the GEM-polymer conjugates were found to form well-defined NPs in aqueous suspension *via* a simple solvent evaporation process and hence the critical aggregation concentration (CAC) was determined using Nile red as a probe that emits fluorescence only in hydrophobic environments[38] (Ex.544 nm, Em.612 nm). The CAC was determined as the sharp fluorescence increase onset above which the polymer forms colloidally stable NPs (Figure S2). It was found that the CAC for two polymer batches with DP 20 and 100, was 0.025 and 0.007 mM, respectively, which is indicative of the interpolymer chain-chain type of self-assembly mechanism that is significantly more pronounced in the longer polymer. The average hydrodynamic diameter (D_h) of the GEM-polymer conjugate NPs of chain length of 100 repeating units was 90 ± 17 nm whereas the D_h of GEM-polymer conjugate NPs of chain length of 20 repeating units was 113 ± 16 nm, as determined by TEM (Figure 3). The D_hs values

measured by DLS were 78.9 nm and 188 nm for GEM-polymer conjugate NPs of chain length of 100 and 20 repeating units

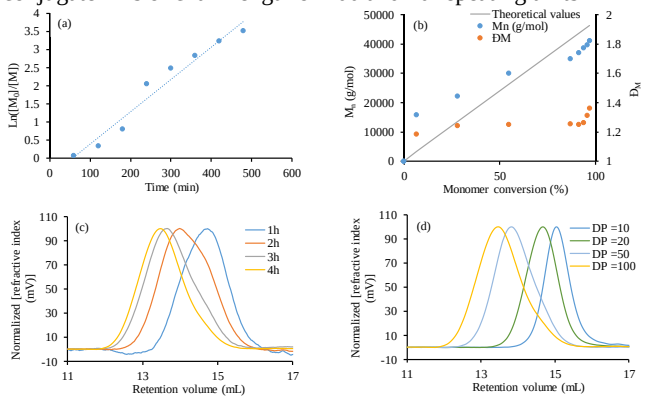

Figure 2. Kinetics of RAFT polymerization of the GEM-monomer conjugate; (a) pseudo first order monomer conversion rate, (b) evolution of M_n and $Đ_M$ as a function of the monomer conversion (determined by ^{1}H NMR spectroscopy), (c) SEC traces of a representative GEM-polymer conjugate at different polymerization times for a targeted DP of 100 and (d) SEC traces of GEM-polymer conjugates of different chain lengths.

respectively (Figure 3). The average D_h value of the GEM-polymer conjugate NPs of chain length of 20 repeating units measured by TEM was significantly lower than the value obtained by DLS possibly due to the dehydration of the samples which leads to significant decrease of the apparent size under TEM; presumably this effect is less observable in the polymer with 100 repeating units owing to the stronger chain-chain interpolymer interactions that lead to a more compact and colloidally stable nanostructure. Furthermore, the possibility of interparticle coagulation in suspension that could lead to higher D_h values should be excluded as the polydispersity (*PDI*) values by DLS were found to be 0.164 and 0.069 for GEM-polymer conjugate NPs of chain length of 100 and 20 repeating units respectively, indicating a narrow average size distribution of the NPs for both polymer batches. As expected, the D_h of GEM-polymer conjugate NPs of chain length of 20 repeating units were larger than GEM-polymer conjugate NPs of chain length of 100 repeating units, due to the more compact structures obtained by the larger polymer, which is in accordance with the lower CAC values. After 13 days in aqueous suspension, the average size of the NPs did not change significantly indicating a relatively good colloidal stability of the NPs in solution (Figure S3). In fact, the D_h of the GEM-polymer conjugate NPs of chain length of 20 repeating units decreased by only 11% after 13 days whereas an increase of the D_h by only 2% of the GEM-polymer conjugate NPs of chain length of 100 repeating units was observed (Figure S3). Furthermore, the *PDI* values were also similar after 13 days, indicating the maintenance of a narrow average size distribution of the NPs in suspension for both polymer batches (Figure S3).

Next, we studied the release of GEM from the GEM-polymer conjugate NPs in PBS (pH 7), sodium acetate buffer (pH 5) and sodium acetate buffer containing Cathepsin B (pH 5) in order to mimic extracellular conditions (i.e. the blood plasma) and the intracellular acidic environment of late endosomes (Figure 4). The profile of GEM release from the GEM-polymer conjugate NPs of different chain lengths were similar indicating no influence of the chain length on the

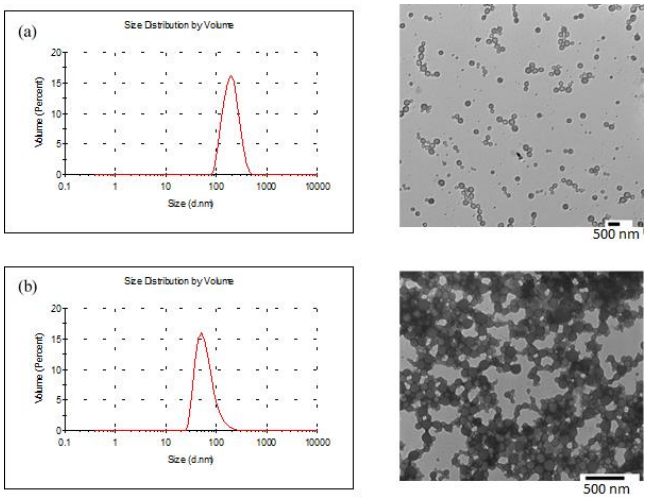

Figure 3. DLS measurements and TEM images of GEM-polymer conjugate NPs; DP (a) 20 and (b) 100.

rate of the hydrolysis of GEM-polymer conjugate (data not shown). Free GEM was liberated rapidly from the dialysis tubing within 1 h in PBS, hence validating the dialysis method to study drug release. GEM was found to be released in a controlled manner throughout the study time in each medium, following a sought-after pseudo zero-order rate which was also observed in other drug-polymer conjugates by Convertine *et al.*.[28] The rate of GEM release was significantly higher at pH 5 compared to pH 7; in fact, 2% and 20% of GEM was released at pH 7 after 1 and 30 days respectively, while at pH 5, 4% and 50% of GEM was released after 1 and 30 days, respectively. The increased rate of GEM release is attributed to the acidic conditions which favor the faster hydrolysis of the ester and the amide link of the GEM-polymer conjugate[39]. Furthermore, the overall rate of GEM release was significantly increased with the addition of Cathepsin B in the sodium acetate buffer (pH 5) since approximatively, 10% and 70% of the drug was released from the GEM-polymer conjugate NPs after 1 and 30 days, respectively, which corroborates our hypothesis that the GEM-polymer conjugate is prone to enzymatic degradation, even in the absence of a cathepsin-specific peptide linker, as has also been shown by other studies[12, 20-21].

The GEM-polymer conjugate NPs were tested *in vitro* against a model pancreatic cell line (MiaPaCa-2) in order to compare their half-maximal inhibitory concentration (IC_{50}) with the parent drug (Figure 5a).The IC_{50} of the latter (GEM), was found to be 450 nM and is consistent with values found in the literature[40]. The IC_{50} of the GEM-monomer conjugate was 2.5 µM which is significantly higher compared to the IC_{50} of GEM. The increase can be explained by the fact that GEM must be released (hydrolyzed) from the polymer backbone to become active. It should be noted that the release rate of GEM should be governed by a two-step hydrolysis mechanism involving an initial hydrolysis of the ester link followed by a second hydrolysis of the amide leading to the corresponding active GEM, which is the target analyte in our HPLC method (see ESI). As expected, similar IC_{50} values were found for the GEM-polymer conjugate NPs for two polymers tested; for DP 100 and 20, the IC_{50} values were 9.5 and 5 µM, respectively. These results are not surprising in that GEM is slowly released from the NPs and hence the effective IC_{50} is somewhat compromised compared to the parent drug. For example, at 72 h incubation time, approximately 16% of GEM is released as evidenced from the drug release curves (Figure 4). It should also be noted that the exact mechanism of the cytotoxic behaviour of the NPs is not trivial to fully elucidate

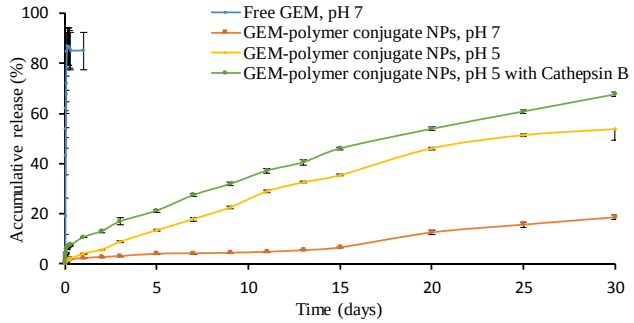

Figure 4. The cumulative release of GEM (%) from the GEM-polymer conjugate (DP 20) as a function of time (days) in PBS (pH ~7), sodium acetate buffer (pH ~5) and sodium acetate buffer containing Cathepsin B (pH ~5); Data show means ±SD from triplicate experiments.

as various factors should be considered: the cellular uptake of the NPs (and potentially its dependence on the average size of each NP batch tested), the cumulative contribution of GEM that has been released extracellularly and intracellularly to the overall cytotoxicity, as well as the possible exocytosis events that could take place under the tested conditions, given the prolonged incubation times. Therefore, we can only limit our analysis on a phenomenological perspective based on the results of the current study.

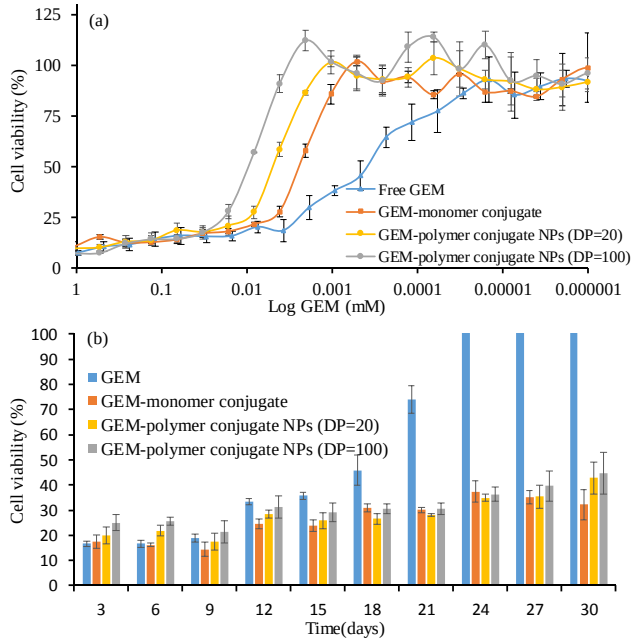

Figure 5. MiaPaCa-2 cells' viability studies with GEM, GEM-monomer and -polymer conjugate NPs (a) as a function of the concentration of GEM, after 72 h of incubation and (b) as a function of time at constant GEM concentration (0.033 mM).

Nevertheless, we were motivated by the slow zero-order release profile of GEM from the NPs and decided to challenge the potentially sustained cytotoxic capacity of the NPs over a prolonged timeframe. We exposed GEM, GEM-monomer, and polymer conjugate NPs at MiaPaCa-2 cells continuously at constant concentrations (Figure S4). Each sample aliquot was incubated with cells for 72 hours before being transferred to freshly plated cells for a total duration of 30 days. It was found that the cytotoxic activity of native GEM against MiaPaCa-2 was compromised after 18 days (ca. 50% of cells survived, Figure 5) and was completely lost after 24 days of treatment. Strikingly, the activity of GEM-monomer and both polymer conjugates NPs was maintained against the cells even for 30 days of treatment (Figure 5b). The prolonged activity of the conjugates is attributed to the slow GEM release, as previously discussed, that could potentially protect the drug from fast chemical degradation as the NPs could act as nanoscale drug depots that exhibit prolonged activity. This result also implies that in an in vivo setting, the NPs could potentially outperform their monomer counterparts due to their improved colloidal stability and the prolonged blood circulation times.

In conclusion, our proposed formulation exhibits certain significant (clinical) advantages that are pragmatically encouraging to proceed in further trials: it is easy to synthesize (and potentially to scale up) and formulate sub-90 nm well-defined nanoparticles, it exhibits very high drug loading per particle (> 50% w/w) and shows more prolonged cytotoxicity compared to the parent drug under the tested conditions. Therefore, we anticipate that our reported findings will pave the way for further *in vivo* studies.

ASSOCIATED CONTENT

Supporting Information. This material is available free of charge *via* the Internet at http://pubs.acs.org.
Experimental details of the synthesis of the GEM-monomer conjugate, its RAFT polymerization and self-assembly protocol. Experimental details of the evaluation of the physical properties of the NPs. ^{1}H, ^{13}C, HSQC, HMBC NMR spectra of GEM-monomer conjugate. CAC measurements, colloidal stability of the NPs and IC_{50} studies on MiaPaCa-2 cells.

AUTHOR INFORMATION

Corresponding Author

*Email: f.joubert@ucl.ac.uk and g.pasparakis@ucl.ac.uk

ACKNOWLEDGMENT

The study was funded by the Engineering and Physical Sciences Research Council (EPSRC, EP/M014649/1; GP, FJ). We thank the UCL Excellence Fellowship award (GP), the Royal Society Wolfson Merit Award (WM130055; SP) and the Monash-Warwick Alliance (LM; SP). We also thank Mr. Adérito J.R. Amaral for helping with the cell culture experiments and Miss Mina Emamzadeh for the development of the HPLC method to quantify GEM in solution.

ABBREVIATIONS

GEM, gemcitabine; D_h, hydrodynamic diameter; CAC, critical aggregation concentration; DP, degree of polymerization; PDI, index of polydispersity; $Đ_M$, Dispersity; CTA, chain transfer agent; RAFT, Reversible Addition-Fragmentation Chain-Transfer; NMR, Nuclear Magnetic Resonance; SEC, Size Exclusion Chromatography; NPs, Nanoparticles; DLS, differential light scattering; TEM, Transmission Electron Macroscopy

REFERENCES

(1) Rahma, O. E.; Duffy, A.; Liewehr, D. J.; Steinberg, S. M.; Greten, T. F. *Ann. Oncol.* **2013,** *24* (8), 1972-1979.
(2) Ansari, D.; Tingstedt, B.; Andersson, B.; Holmquist, F.; Sturesson, C.; Williamsson, C.; Sasor, A.; Borg, D.; Bauden, M.; Andersson, R. *Future Oncol.* **2016,** *12* (16), 1929-1946.
(3) Oettle, H.; Neuhaus, P.; Hochhaus, A.; Hartmann, J. T.; Gellert, K.; Ridwelski, K.; Niedergethmann, M.; Zülke, C.; Fahlke, J.; Arning, M. B.; Sinn, M.; Hinke, A.; Riess, H. *JAMA* **2013,** *310* (14), 1473-1481.

(4) Galmarini, C. M.; Mackey, J. R.; Dumontet, C. *Leukemia* **2001,** *15* (6), 875-90.
(5) Andersson, R.; Aho, U.; Nilsson, B. I.; Peters, G. J.; Pastor-Anglada, M.; Rasch, W.; Sandvold, M. L. *Scand. J. Gastroenterol.* **2009,** *44* (7), 782-786.
(6) Santini, D.; Schiavon, G.; Vincenzi, B.; Cass, C. E.; Vasile, E.; Manazza, A. D.; Catalano, V.; Baldi, G. G.; Lai, R.; Rizzo, S.; Giacobino, A.; Chiusa, L.; Caraglia, M.; Russo, A.; Mackey, J.; Falcone, A.; Tonini, G. *Curr. Cancer Drug Targets* **2011,** (11), 123-129.
(7) Lostao, M. P.; Mata, J. F.; Larrayoz, I. M.; Inzillo, S. M.; Casado, F. J.; Pastor-Anglada, M. *FEBS Lett.* **2000,** *481* (2), 137-140.
(8) Rauchwerger, D. R.; Firby, P. S.; Hedley, D. W.; Moore, M. J. *Cancer Res.* **2000,** *60* (21), 6075-6079.
(9) Galmarini, C. M.; Thomas, X.; Calvo, F.; Rousselot, P.; El Jafaari, A.; Cros, E.; Dumontet, C. *Leuk. Res.* **2002,** *26* (7), 621-629.
(10) Moysan, E.; Bastiat, G.; Benoit, J.-P. *Mol. Pharm.* **2013,** *10* (2), 430-444.
(11) Weiss, J. T.; Dawson, J. C.; Fraser, C.; Rybski, W.; Torres-Sánchez, C.; Bradley, M.; Patton, E. E.; Carragher, N. O.; Unciti-Broceta, A. *J. Med. Chem.* **2014,** *57* (12), 5395-5404.
(12) Xu, Y.; Geng, J.; An, P.; Xu, Y.; Huang, J.; Lu, W.; Liu, S.; Yu, J. *RSC Adv.* **2015,** *5* (9), 6985-6992.
(13) Khare, V.; Sakarchi, W. A.; Gupta, P. N.; Curtis, A. D. M.; Hoskins, C. *RSC Adv.* **2016,** *6* (65), 60126-60137.
(14) Han, H.; Jin, Q.; Wang, Y.; Chen, Y.; Ji, J. *Chem. Commun.* **2015,** *51* (98), 17435-17438.
(15) Schroeder, A.; Heller, D. A.; Winslow, M. M.; Dahlman, J. E.; Pratt, G. W.; Langer, R.; Jacks, T.; Anderson, D. G. *Nat. Rev. Cancer* **2012,** *12* (1), 39-50.
(16) Fang, J.; Nakamura, H.; Maeda, H. *Adv. Drug Deliv. Rev.* **2011,** *63* (3), 136-151.
(17) Zhong, Y.; Meng, F.; Deng, C.; Zhong, Z. *Biomacromolecules* **2014,** *15* (6), 1955-1969.
(18) Danhier, F.; Feron, O.; Préat, V. *J. Control. Release* **2010,** *148* (2), 135-146.
(19) Trung Bui, D.; Maksimenko, A.; Desmaële, D.; Harrisson, S.; Vauthier, C.; Couvreur, P.; Nicolas, J. *Biomacromolecules* **2013,** *14* (8), 2837-2847.
(20) Wang, W.; Li, C.; Zhang, J.; Dong, A.; Kong, D. *J. Mater. Chem. B* **2014,** *2* (13), 1891-1901.
(21) Chitkara, D.; Mittal, A.; Behrman, S. W.; Kumar, N.; Mahato, R. I. *Bioconjugate Chemistry* **2013,** *24* (7), 1161-1173.
(22) Khare, V.; Kour, S.; Alam, N.; Dubey, R. D.; Saneja, A.; Koul, M.; Gupta, A. P.; Singh, D.; Singh, S. K.; Saxena, A. K.; Gupta, P. N. *Int. J. Pharm.* **2014,** *470* (1–2), 51-62.
(23) Song, H.; Xiao, H.; Zheng, M.; Qi, R.; Yan, L.; Jing, X. *J. Mater. Chem. B* **2014,** *2* (38), 6560-6570.
(24) Vandana, M.; Sahoo, S. K. *Biomaterials* **2010,** *31* (35), 9340-9356.
(25) Liang, T.-J.; Zhou, Z.-M.; Bao, Y.-Q.; Ma, M.-Z.; Wang, X.-J.; Jing, K. *Int. J. Pharm. 513* (1-2), 564-571.
(26) Das, A.; Theato, P. *Chem. Rev.* **2016,** *116* (3), 1434-1495.
(27) Son, H. N.; Srinivasan, S.; Yhee, J. Y.; Das, D.; Daugherty, B. K.; Berguig, G. Y.; Oehle, V. G.; Kim, S. H.; Kim, K.; Kwon, I. C.; Stayton, P. S.; Convertine, A. J. *Polym. Chem.* **2016,** *7* (27), 4494-4505.
(28) Das, D.; Srinivasan, S.; Kelly, A. M.; Chiu, D. Y.; Daugherty, B. K.; Ratner, D. M.; Stayton, P. S.; Convertine, A. J. *Polym. Chem.* **2016,** *7* (4), 826-837.
(29) Yang, J.; Luo, K.; Pan, H.; Kopečková, P.; Kopeček, J. *React. Funct. Polym.* **2011,** *71* (3), 294-302.
(30) Larson, N.; Yang, J.; Ray, A.; Cheney, D. L.; Ghandehari, H.; Kopeček, J. *Int. J. Pharm.* **2013,** *454* (1), 435-443.
(31) Zhang, R.; Yang, J.; Sima, M.; Zhou, Y.; Kopeček, J. *Proc. Natl. Acad. Sci. U.S.A.* **2014,** *111* (33), 12181-12186.
(32) Zhou, G.-J.; Li, X.; Teng, M.-X.; Chu, G.-H.; Lin, X.-F. *J. Appl. Polym. Sci.* **2012,** *124* (3), 1840-1847.
(33) Lai, H.; Lu, M.; Lu, H.; Stenzel, M. H.; Xiao, P. *Polym. Chem.* **2016,** *7*, 6220-6230.
(34) Parrott, M. C.; Finniss, M.; Luft, J. C.; Pandya, A.; Gullapalli, A.; Napier, M. E.; DeSimone, J. M. *J. Am. Chem. Soc.* **2012,** *134* (18), 7978-7982.
(35) Boyer, C.; Bulmus, V.; Davis, T. P.; Ladmiral, V.; Liu, J.; Perrier, S. *Chem. Rev.* **2009,** *109* (11), 5402-5436.
(36) Theis, A.; Feldermann, A.; Charton, N.; Stenzel, M. H.; Davis, T. P.; Barner-Kowollik, C. *Macromolecules* **2005,** *38* (7), 2595-2605.
(37) *Handbook of RAFT Polymerization*; Barner-Kowollik, C., Eds.; John Wiley and Sons: Germany, 2008.
(38) Gillies, E. R.; Jonsson, T. B.; Fréchet, J. M. J. *J Am Chem Soc* **2004,** *126* (38), 11936-11943.
(39) D'Souza, A. J. M.; Topp, E. M. *J. Pharm. Sci.* **2004,** *93* (8), 1962-1979.
(40) Awasthi, N.; Zhang, C.; Schwarz, A. M.; Hinz, S.; Wang, C.; Williams, N. S.; Schwarz, M. A.; Schwarz, R. E. *Carcinogenesis* **2013,** *34* (10), 2361-2369.